epl A Letters Journal Exploring the Frontiers of Physics

October 2008

EPL, **84** (2008) 10012
doi: 10.1209/0295-5075/84/10012

www.epljournal.org

Single-particle hydrodynamics in DPD: A new formulation

W. Pan[1], I. V. Pivkin[1,2] and G. E. Karniadakis[1(a)]

[1] *Division of Applied Mathematics, Brown University - Providence, RI 02912 USA*
[2] *Department of Materials Science and Engineering, Massachusetts Institute of Technology Cambridge, MA 02139 USA*

received 18 June 2008; accepted in final form 28 August 2008
published online 26 October 2008

PACS 02.70.Ns – Molecular dynamics and particle methods
PACS 05.20.Jj – Statistical mechanics of classical fluids
PACS 83.10.Rs – Computer simulation of molecular and particle dynamics

Abstract – We present a new formulation of dissipative particle dynamics (DPD) that leads to correct hydrodynamics in flows around bluff bodies represented by a single particle. In particular, we introduce a shear drag coefficient and a corresponding term in the dissipative force, which along with the angular momentum incorporate non-central shear forces between particles and preserve angular momentum. We consider several prototype flows to verify the performance of the proposed formulation with comparisons against theoretical and continuum-based simulation results. Our method is similar to the Fluid Particle Method (FPM) of Espanol (*Phys. Rev. E*, **57** (1998) 2930) and it has the computational and implementation simplicity of the standard DPD approach.

Introduction. – In molecular and mesoscopic particle-based simulations of flows past spheres or any other bluff bodies, the bodies are typically represented by hundreds of particles. For example, in DPD simulations of flow past a single sphere reported in [1], 500 particles were employed to represent the sphere in order to obtain the correct hydrodynamics, and hence the correct value of the drag force. In biological flows in small arteries where explicit modeling of red blood cells (RBCs) is often required, spectrin-level models employ more than 20000 particles to represent a single RBC [2]. Such multi-particle representations may render a simulation prohibitively expensive. For example, in an arteriole of $50\,\mu$m diameter ($500\,\mu$m length) with 35% of volume occupied by RBCs, we would require 10^8 unknowns for modeling RBCs and *hundreds of millions* of particles to represent the flow. On the other hand, in DPD simulations of polymeric and colloidal solutions, the polymer beads and colloidal particles are typically represented by *single* DPD particles [3,4], which makes such simulations very efficient. However, the single DPD particles are subject to central pairwise forces only, effectively ignoring the non-central shear forces between dissipative particles.

This defficiency of DPD has been recognized in the past by Espanol and collaborators [5–7], who proposed the fluid particle model (FPM) [5]. Compared to standard DPD method [8–10], this model incorporates two additional *non-central* shear components into the dissipative forces, which are coupled to the random forces by means of the fluctuation-dissipative theorem. FPM can be considered as generalization of the DPD method that includes torques and angular velocities of the particles, and it conserves both linear and angular momenta.

More specifically, a FPM simulation consists of a collection of particles of mass m with positions $\mathbf{r}_i$ and angular velocities $\mathbf{\Omega}_i$. We define $\mathbf{r}_{ij} = \mathbf{r}_i - \mathbf{r}_j$, $r_{ij} = |\mathbf{r}_{ij}|$, $\mathbf{e}_{ij} = \mathbf{r}_{ij}/r_{ij}$, $\mathbf{v}_{ij} = \mathbf{v}_i - \mathbf{v}_j$. The force and torque on particle i are given by

$$\begin{aligned} \mathbf{F}_i &= \sum_j \mathbf{F}_{ij}, \\ \mathbf{T}_i &= -\sum_j \frac{\mathbf{r}_{ij}}{2} \times \mathbf{F}_{ij}, \end{aligned} \tag{1}$$

where the force that particle j exerts on particle i is given by

$$\mathbf{F}_{ij} = \mathbf{F}_{ij}^C + \mathbf{F}_{ij}^T + \mathbf{F}_{ij}^R + \widetilde{\mathbf{F}}_{ij}. \tag{2}$$

The conservative (C), translational (T), rotational (R), and random (tilde) components are given, respectively, by

$$\mathbf{F}_{ij}^C = -V'(r_{ij})\mathbf{e}_{ij}, \tag{3}$$

$$\mathbf{F}_{ij}^T = -\gamma_{ij} m \mathbf{T}_{ij} \cdot \mathbf{v}_{ij}, \tag{4}$$

$$\mathbf{F}_{ij}^R = -\gamma_{ij} m \mathbf{T}_{ij} \cdot \left[\frac{\mathbf{r}_{ij}}{2} \times (\mathbf{\Omega}_i + \mathbf{\Omega}_j) \right], \tag{5}$$

(a) E-mail: gk@dam.brown.edu

$$\widetilde{\mathbf{F}}_{ij}dt = (2k_BT\gamma_{ij}m)^{1/2} \times \left[\widetilde{A}(r_{ij})\overline{d\mathbf{W}^S_{ij}} + \widetilde{B}(r_{ij})\frac{1}{d}\mathrm{tr}[d\mathbf{W}_{ij}]\mathbf{1} + \widetilde{C}(r_{ij})d\mathbf{W}^A_{ij}\right]\cdot\mathbf{e}_{ij}. \quad (6)$$

In FPM, the conservative force is the same as in the standard DPD approach that employs a quadratic potential $V(r_{ij})$, *i.e.*,

$$\mathbf{F}^C_{ij} = a\left(1-\frac{r_{ij}}{r_c}\right)\mathbf{e}_{ij}, \quad (7)$$

with r_c being the cut-off distance set to $r_c = 1$. The matrix $\mathbf{T}_{ij}$ in the rotational force is given by

$$\mathbf{T}_{ij} = A(r_{ij})\mathbf{1} + B(r_{ij})\mathbf{e}_{ij}\mathbf{e}_{ij}, \quad (8)$$

with

$$\begin{aligned} A(r) &= \frac{1}{2}\left[\widetilde{A}^2(r) + \widetilde{C}^2(r)\right], \\ B(r) &= \frac{1}{2}\left[\widetilde{A}^2(r) - \widetilde{C}^2(r)\right] + \frac{1}{d}\left[\widetilde{B}^2(r) - \widetilde{A}^2(r)\right], \end{aligned} \quad (9)$$

where $\widetilde{A}(r)$, $\widetilde{B}(r)$, $\widetilde{C}(r)$ are scalar functions. For $\widetilde{A}(r) = \widetilde{C}(r) = 0$ the standard DPD scheme is recovered, in which only central forces remain while torques vanish. Hence, FPM can be indeed recognized as a generalization of the standard DPD method. The scalar functions commonly employed in FPM simulations are [4,11]:

$$\begin{aligned} &\widetilde{A}(r) = 0, \\ &A(r) = B(r) = [f(r)]^2 = \left(1-\frac{r}{r_c}\right)^2. \end{aligned} \quad (10)$$

The random force includes symmetric, antisymmetric and traceless noise matrices defined as

$$\begin{aligned} d\mathbf{W}^{S\mu\nu}_{ij} &= \frac{1}{2}(d\mathbf{W}^{\mu\nu}_{ij} + d\mathbf{W}^{\nu\mu}_{ij}), \\ d\mathbf{W}^{A\mu\nu}_{ij} &= \frac{1}{2}(d\mathbf{W}^{\mu\nu}_{ij} - d\mathbf{W}^{\nu\mu}_{ij}), \\ \overline{d\mathbf{W}^S_{ij}} &= d\mathbf{W}^S_{ij} - \frac{1}{d}\mathrm{tr}[d\mathbf{W}^S_{ij}]\mathbf{1}, \end{aligned} \quad (11)$$

where $d\mathbf{W}^{\mu\nu}_{ij}$ is a matrix of independent Wiener increments, which is assumed to be symmetric under particle interchange. The parameter d is the physical dimension of space and is set to $d = 3$.

Dynamical and rheological properties of colloidal suspensions in simple fluid solvents were successfully simulated using FPM in [4]. Each colloidal particle was represented by a single FPM particle and the conservative forces for solvent-colloid and colloid-colloid interactions were derived from Lennard-Jones potentials. Unfortunately, the drag force and torque on a solid sphere represented by a single FPM particle in the above formulation does not match the theoretical and experimental values.

In this paper, we present a new formulation of the FPM equations which deviates only slightly from the standard DPD approach. The resulting method can provide quantitatively correct hydrodynamic forces *and* torques for a single spherical particle. The new formulation can be readily employed in a wide range of applications, including studies of properties of colloidal suspensions as well as in coarse-grained simulations of polymer solutions or even in dense suspension of RBCs with reduced deformability, *e.g.*, in simulating malaria-infected RBCs [12].

New formulation. – A single particle in FPM experiences both a drag force *and* a torque whose magnitudes are controlled by the parameter γ_{ij} in eqs. (4) and (5). Simulation results suggest that these forces are not balanced properly, and hence we cannot obtain the correct hydrodynamics for a single particle. The idea behind the new formulation is to modify the FPM equations in such way that the forces acting on a particle can be *explicitly* divided into two separate components: *central* and *shear* (non-central) components. This allows us to redistribute and hence balance the forces acting on a single particle to obtain the correct hydrodynamics. Specifically, the new formulation is a modification of the FPM formulation described in the previous section, and is defined by the following choice of the functions $\widetilde{A}(r)$, $\widetilde{B}(r)$ and $\widetilde{C}(r)$:

$$\begin{aligned} \widetilde{A}(r) &= 0, \\ A(r) &= \gamma^S[f(r)]^2, \\ B(r) &= (\gamma^C - \gamma^S)[f(r)]^2. \end{aligned} \quad (12)$$

Here again $f(r) = 1 - \frac{r}{r_c}$ is the weight function and r_c is the cut-off radius while the superscripts C and S denote the "central" and "shear" components, respectively. This notation can be clarified further if we look at the particle forces. Specifically, the *translational force* is given by

$$\begin{aligned} \mathbf{F}^T_{ij} &= -\left[\gamma^S_{ij}f^2(r)\mathbf{1} + (\gamma^C_{ij} - \gamma^S_{ij})f^2(r)\mathbf{e}_{ij}\mathbf{e}_{ij}\right]\cdot\mathbf{v}_{ij} = \\ &\quad -\gamma^C_{ij}f^2(r_{ij})(\mathbf{v}_{ij}\cdot\mathbf{e}_{ij})\mathbf{e}_{ij} - \gamma^S_{ij}f^2(r_{ij}) \\ &\quad \times\left[\mathbf{v}_{ij} - (\mathbf{v}_{ij}\cdot\mathbf{e}_{ij})\mathbf{e}_{ij}\right]. \end{aligned} \quad (13)$$

It accounts for the drag due to the relative translational velocity $\mathbf{v}_{ij}$ of particles i and j. This force can be decomposed into two components: one along and the other one perpendicular to the lines connecting the centers of the particles. Hence, the corresponding drag coefficients are denoted by γ^C_{ij} and γ^S_{ij} for the "*central*" and the "*shear*" components, respectively. We note here that the central component of the force is exactly the same as the dissipative force in the standard DPD approach.

The *rotational force* is defined by

$$\mathbf{F}^R_{ij} = -\gamma^S_{ij}f^2(r_{ij})\left[\frac{\mathbf{r}_{ij}}{2}\times(\mathbf{\Omega}_i + \mathbf{\Omega}_j)\right]. \quad (14)$$

Finally, the *random force* is given by

$$\widetilde{\mathbf{F}}_{ij}dt = f(r_{ij})\left[\frac{1}{\sqrt{3}}\sigma^C_{ij}\mathrm{tr}[d\mathbf{W}_{ij}]\mathbf{1} + \sqrt{2}\sigma^S_{ij}d\mathbf{W}^A_{ij}\right]\cdot\mathbf{e}_{ij}, \quad (15)$$

where $\sigma_{ij}^S = \sqrt{2k_BT\gamma_{ij}^S}$ and $\sigma_{ij}^C = \sqrt{2k_BT\gamma_{ij}^C}$. We recommend the use of the generalized weight function $f(r) = (1-\frac{r}{r_c})^s$ with $s=0.25$ [13] in eqs. (13)–(15); our numerical results show higher accuracy with $s=0.25$ compared to the typical choice $s=1$. The standard DPD method is recovered when $\gamma_{ij}^S \equiv 0$, *i.e.*, when the shear components of the forces are ignored.

In simulations of complex fluids the values of the drag coefficients γ_{ij}^C and γ_{ij}^S can vary for different types of particles. For example, in polymer simulations when one bead represents a collection of atoms, these coefficients can be specified to achieve the desired values of drag and torque on the individual beads. To illustrate this concept we will consider here a system in which a spherical (colloidal) particle is represented by a single DPD particle. We will adjust the coefficients γ_{ij}^C and γ_{ij}^S so that both the drag force and the torque exerted on the colloidal particle in flow simulations correspond to the stick (no-slip) conditions on its surface. To this end, we first consider two (low Reynolds number) flow simulations: 1) unbounded flow around a sphere *rotating* at a constant angular velocity without translation; 2) unbounded uniform flow around a *fixed* sphere. Once the values of γ_{ij}^C and γ_{ij}^S are defined, we will perform additional simulations to verify the performance of the new model.

In all simulations reported in this paper the parameters for the fluid particles are $\rho=3$, $a=25$, $\gamma_{ff}^C = \gamma_{ff}^S = 4.5$ and σ_{ij}^C and σ_{ij}^S are computed based on the relationships derived from the fluctuation-dissipation theorem. We aim to determine the proper values of γ_{cf}^C and γ_{cf}^S. (Here "c" and "f" refer to "colloidal" and "fluid", respectively.) We first study low Reynolds number flow around a sphere, which is represented by a single DPD particle; to distinguish this particle from the fluid particles we will refer to it as "colloidal" particle. Even though the interaction forces are non-zero within a spherical region of radius $r_c=1$ surrounding the particle, the colloidal particle represents a sphere with radius $R<r_c$. This effective radius is found using the Stokes-Einstein relation [14], *i.e.*,

$$D = \frac{k_BT}{c\pi\mu R}, \tag{16}$$

where D is the diffusion coefficient of the particle, k_BT is the temperature of the system, and μ is the viscosity of the fluid. Also, c is a constant determined by the choice of hydrodynamic boundary conditions on the surface of the particle; for stick (no-slip) conditions the constant c is equal to 6, while for slip boundary conditions $c=4$; we set $c=6$ here. The viscosity μ of the fluid is found to be 3.6388 using the method described in [15]. The diffusion coefficient $D=0.0533$ is calculated from the mean-square displacement, *i.e.*,

$$D = \lim_{t\to\infty} \frac{\langle[\mathbf{r}(t)-\mathbf{r}(0)]^2\rangle}{6t}, \tag{17}$$

where $\langle\cdot\rangle$ is an ensemble average, t is time and $\mathbf{r}$ is the position vector of the particle. The effective radius of the colloidal particle is found to be $R=0.2737r_c$. We note here that the effective radius is not sensitive to the specific choice of the parameters γ_{ij}^C and γ_{ij}^S, but it mainly depends on the conservative forces used in the model. We have verified this through extensive numerical simulations with different values of the model parameters.

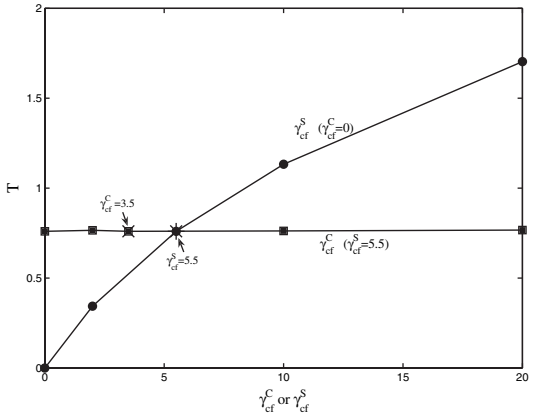

Fig. 1: Dependence of torque on the sphere exerted by the fluid on the value of: 1) γ_{cf}^S when $\gamma_{cf}^C=0$, and: 2) γ_{cf}^C when $\gamma_{cf}^S=5.5$. Here $\Omega=-0.4$.

Once the effective radius is determined, we proceed by obtaining the drag coefficients for the colloidal/fluid particle interactions. We start with simulations of the flow around a single colloidal particle with fixed position and constant angular velocity Ω. The particle is located at the center of a box ($10r_c \times 10r_c \times 10r_c$) with periodic boundary conditions. The angular velocity is specified so that the Reynolds number is low ($Re=0.0247$). In Stokes flow in an unbounded domain, the torque on the sphere is given by [16]

$$T = -8\pi\mu\Omega R^3. \tag{18}$$

We assume that eq. (18) is a good approximation of the torque that our colloidal particle should experience. Based on this we adjust the shear drag coefficient γ_{cf}^S (set $\gamma_{ff}^C = \gamma_{ff}^S = 4.5$) in the model, so that the computed torque is equal to Stokes flow prediction. By setting $\gamma_{cf}^C=0$ we investigate the dependence of the torque on the value of γ_{cf}^S. We find that $\gamma_{cf}^S=5.5$ gives us a torque which is within 1.3% the Stokes prediction. The torque experienced by the colloidal particle in this flow is positively correlated to γ_{cf}^S but is not sensitive to the particular value of γ_{cf}^C as the central drag force does not contribute to the torque in our model. This was verified in the numerical simulations and is illustrated in fig. 1.

Next we simulate uniform flow past a *periodic array* of spheres. One sphere, represented by a single (colloidal) DPD particle, is fixed (no rotation or translation) at the center of periodic domain. The flow is driven by an external body force F_{ext} applied to the fluid particles. The Reynolds number in the simulations is small, $Re=0.033$, and the volume fraction is 8.588×10^{-5}. The drag force on

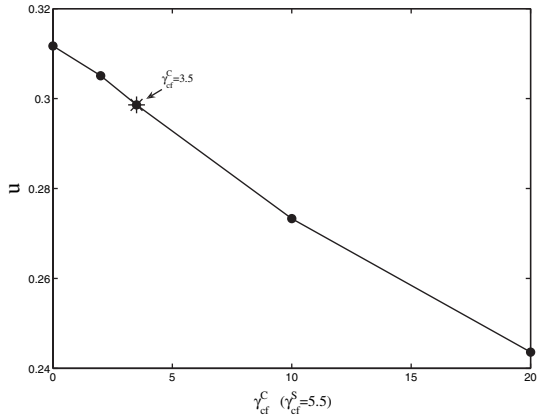

Fig. 2: Dependence of the superficial velocity of the fluid on the value of γ^C_{cf} when $\gamma^S_{cf} = 5.5$ in the unbounded uniform Stokes flow around one sphere.

a periodic array of spheres at low volume fraction in low Reynolds number flow can be approximated by

$$F_{ext} = 6\pi\mu u R, \tag{19}$$

where u is the superficial velocity of the fluid defined as

$$u = \frac{1}{V}\int_V v \mathrm{d}V. \tag{20}$$

It can be shown that the sedimentation velocity of an array of bodies under the action of a constant force is equal to this superficial velocity [17]. With fixed value of $\gamma^S_{cf} = 5.5$ obtained earlier, we adjust the central drag force coefficient γ^C_{cf} so that the simulation results satisfy eq. (19). The dependence of the superficial velocity on γ^C_{cf} is shown in fig. 2. We find that $\gamma^C_{cf} = 3.5$ gives superficial velocity $u = 0.2986$, which is within 1.2% from the value in eq. (20).

Remark: We note that the values of coefficients $\gamma^C_{cf} = 3.5$ and $\gamma^S_{cf} = 5.5$ for colloidal/fluid particles interactions, which we obtained through numerical simulations, satisfy the relation $\gamma^C_{cf} + \gamma^S_{cf} = \gamma^C_{ff} + \gamma^S_{ff}$, where $\gamma^C_{ff} = \gamma^S_{ff} = 4.5$ are the coefficients used for the fluid/fluid particle interactions. This relation seems to hold for other choices of fluid/fluid coefficients as we verified in several numerical simulations. For example, for $\gamma^C_{ff} = \gamma^S_{ff} = 2.0$, we find $\gamma^C_{cf} = 1.0$ and $\gamma^S_{cf} = 3.0$, while for $\gamma^C_{ff} = \gamma^S_{ff} = 8.0$, we have $\gamma^C_{cf} = 7.0$ and $\gamma^S_{cf} = 9.0$. In this intriguing relation, our choice of $\gamma^C_{ff} = \gamma^S_{ff}$ is consistent with the *incompressible* formulation in [6,7] (eq. (12)) in the absence of any angular variables. However, in our case we include the angular variables and hence we cannot provide a rigorous theoretical justification at the present time.

Simulation results. – In the previous section we presented the new DPD formulation, defined the effective radius of colloidal particle R using the Stokes-Einstein relation, and calibrated the central and shear drag force coefficients, $\gamma^S_{cf} = 5.5$ and $\gamma^C_{cf} = 3.5$, so that at low Reynolds numbers the new model produces results with desired drag and torque on a single colloidal particle. In this section, we apply the model to three prototype (low Reynolds number) flow problems: (1) sphere in Couette flow, (2) sphere in Poiseuille flow, and (3) flow past two spheres. In all cases we set $\gamma^S_{cf} = 5.5$ and $\gamma^C_{cf} = 3.5$, and we compare the simulation results with available theoretical results. In addition, we consider the rotation of a linear chain of spheres around its major axis for which available Multipole Expansion Method (MEM) and Boundary Element Method (BEM) results are used for comparison.

Table 1: Couette flow: values of torque when applying different Ω and v from the simulations (T_{sim}) compared with the theoretical results (T_{the}).

Ω	$\frac{1}{2}(\nabla \times v)$	T_{sim}	T_{the}	Error
0	0.2	0.3675	0.3750	2.0%
0	0.4	0.7540	0.7500	0.5%
−0.2	0.2	0.7289	0.7500	2.8%
−0.2	0.4	1.0659	1.1251	5.3%

Couette flow around a sphere. Let us consider a sphere rotating with constant angular velocity in Couette flow. At low Reynolds numbers the torque on the sphere can be approximated by the Stokes flow solution [16]

$$T = 8\pi\mu R^3\left[\frac{1}{2}(\nabla \times v) - \Omega\right]. \tag{21}$$

In our simulations the flow domain is a box ($15r_c \times 6r_c \times 8r_c$), periodic in x and y directions while the two walls bounding the fluid domain in the z-direction are modeled as in [18]. The walls are moving with the velocity of the same magnitude v in opposite directions. A sphere, modeled by a single particle, is fixed at the center of the domain and is rotating with prescribed constant angular velocity Ω. Comparison of the calculated torque on the sphere with values given by eq. (21) for four different simulations are listed in table 1. The Reynolds number in simulations is low (maximum Re is 0.0371). The DPD results are within a few percent from the Stokes flow predictions.

Poiseuille flow around a sphere. According to [16], the drag and torque on a sphere held stationary between two planar walls in pressure-driven Poiseuille flow at low Reynolds number are given by

$$\begin{aligned} F &= 6\pi\mu u_h R\left[\frac{1-\dfrac{R^2}{9h^2}}{1-0.6526\dfrac{R}{h}+0.3160\dfrac{R^3}{h^3}-0.242\dfrac{R^4}{h^4}}\right], \\ T &= \frac{8}{3}\pi\mu u_h \frac{R^3}{h}\left[1+0.0758\frac{R}{h}+0.049\frac{R^2}{h^2}\right], \end{aligned} \tag{22}$$

where u_h is the velocity at the location of the center of the sphere in the Poiseuille flow without sphere, and h is

Table 2: Drag force F_{sim} and torque T_{sim} exerted on the sphere by the fluid in Poiseuille flow with three different pressure gradients, compared with the theoretical results F_{the} and T_{the} calculated using eq. (22).

Re	F_{sim}	F_{the}	Error	T_{sim}	T_{the}	Error
0.0491	4.4881	5.114	4.6%	0.0838	0.0786	6.6%
0.0993	9.689	10.230	5.3%	0.163	0.157	3.8%
0.201	18.881	20.463	7.7%	0.313	0.315	0.6%

the distance from the center of the sphere to the nearest wall divided by the distance between the walls.

In DPD simulations, the flow domain is a box of size $15r_c$, $6r_c$ and $8r_c$ in x, y and z directions, respectively. The system is periodic in the x and y directions. The two walls bounding the fluid in z-direction are modeled as in [19]. One colloidal particle is placed $h = 2r_c$ away from the wall and held fixed during the simulations. An external body force F_{ext} is applied to fluid particles in the x-direction to drive the flow. Simulation results and theoretical predictions based on (22) are listed in table 2.

Flow past two spheres. We now consider Stokes flow past a pair of spheres of radius R. The spheres are fixed and are not allowed to rotate, and the direction of the flow is normal to the line connecting the centers of the spheres. The drag force and torque on each of the spheres are given by [16]

$$F = 6\pi\mu R u\left(1 - \frac{3R}{4l} + \frac{9R^2}{16l^2} - \frac{59R^3}{64l^3} + \frac{465R^4}{256l^4} - \frac{15813R^5}{7168l^5}\right),$$
$$T = 8\pi\mu R^3 u\left(\frac{3R}{4l^2} - \frac{9R^2}{16l^3} + \frac{27R^3}{64l^4} - \frac{273R^4}{256l^5} + \frac{1683R^5}{1024l^6}\right), \tag{23}$$

where l is the distance between spheres, and u is superficial velocity.

In DPD simulations, two colloidal particles are placed in the middle of the computational domain of size $30r_c \times 30r_c \times 30r_c$, periodic in all directions. The flow is driven by an external force applied to the fluid particles. The maximum Reynolds number is equal to $Re = 0.0756$. Comparison of the drag force and torque obtained in simulations with the Stokes flow predictions based on (23) are listed in table 3.

Rotation of a linear chain of spheres around its major axis. Finally, we consider a linear chain of spheres rotating in the fluid around its axis with constant angular velocity. The spheres contact each other. A dimensionless shape factor for the torque exerted by the fluid on the chain is equal to [20]

$$T_s = -\frac{T}{8\pi\mu\Omega N R^3}, \tag{24}$$

where T is the total torque exerted on the chain.

Table 3: Drag force F_{sim} and torque T_{sim} on each sphere exerted by the fluid in the simulations with three different values of l, compared with the theoretical results F_{the} and T_{the}.

l	F_{sim}	F_{the}	Error	T_{sim}	T_{the}	Error
2.0	4.861	5.100	4.7%	0.0253	0.0261	3.1%
1.5	4.857	5.089	4.6%	0.0451	0.0463	2.6%
1.0	4.863	5.185	6.2%	0.113	0.106	6.6%

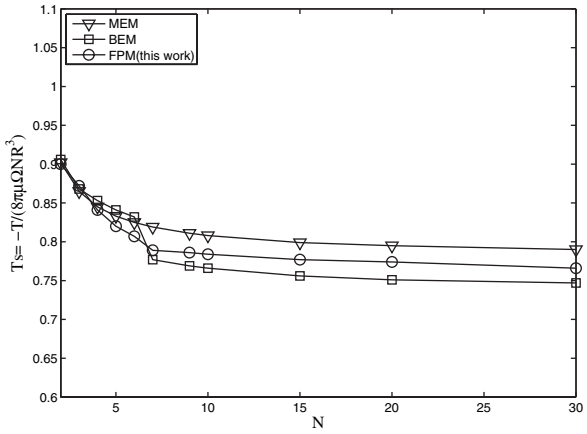

Fig. 3: Dimensionless shape factor T_s of torque for the rotation of a straight chain of N spheres around its major axis.

Figure 3 shows comparison of our results with results obtained using the Multipole Expansion Method (MEM) [20] and the Boundary Element Method (BEM) [21]. In MEM the flow velocity is represented by a series of spherical harmonics centered at the individual spheres, while in BEM the sphere surfaces are represented explicitly by a mesh. The simulation results are in good agreement with both methods, with a maximum difference of 3.7%.

Summary. – We have developed a simple and efficient formulation of DPD that will allow simulation of polymeric and colloidal solutions as well as flows past bluff bodies by representing the solid beads or particles by single dissipative particles. In all cases tested the accuracy of the drag force and torque was good and comparable to the case where hundreds of DPD particles are employed to represent a colloidal particle. The statistical uncertainty in all the results presented in the tables was less than 0.5%. In particular, the smaller is the Reynolds number the better is the agreement with the theoretical results. To this end, a modified weight function is recommended that enhances the viscosity of the DPD fluid. For non-spherical objects a few DPD particles can be employed to accommodate the geometric shape. The new method leads to good results in colloidal suspensions as torque is important to obtain the right viscosity in dense concentrations [4]. It will also be interesting to study polymeric solutions with the new method, where the individual beads in a given chain are allowed to rotate unlike the simulations using the standard DPD approach [3].

* * *

This work was supported by the NSF/IMAG, and computations were performed on the Ranger at TACC, an NSF supercomputing center.

REFERENCES

[1] Chen S., Phan-Thien N., Khoo B. C. and Fan X. J., *Phys. Fluids*, **18** (2006) 103605.
[2] Li J., Dao M., Lim C. T. and Suresh S., *Biophys. J.*, **88** (2005) 3707.
[3] Symeonidis V., Caswell B. and Karniadakis G., *Phys. Rev. Lett.*, **95** (2005) 076001.
[4] Pryamitsyn V. and Ganesan V., *J. Chem. Phys.*, **122** (2005) 104906.
[5] Espanol P., *Phys. Rev. E*, **57** (1998) 2930.
[6] Espanol P., *Europhys. Lett.*, **39** (1997) 605.
[7] Espanol P. and Revenga M., *Phys. Rev. E*, **67** (2003) 026705.
[8] Hoogerbrugge P. J. and Koelman J. M. V. A., *Europhys. Lett.*, **19** (1992) 155.
[9] Espanol P. and Warren P., *Europhys. Lett.*, **30** (1995) 191.
[10] Groot R. D. and Warren P. B., *J. Chem. Phys.*, **107** (1997) 4423.
[11] Dzwinel W. and Yuen D. A., *J. Colloid Interface Sci.*, **247** (2002) 463.
[12] Suresh S., *J. Mater. Res.*, **21** (2006) 1871.
[13] Fan X. J., Phan-Thien N., Chen S., Wu X. H. and Ng T. Y., *Phys. Fluids* , **18** (2006) 063102.
[14] Schmidt J. R. and Skinner J. L., *J. Phys. Chem. B*, **108** (2004) 6767.
[15] Backer J. A., Lowe C. P., Hoefsloot H. C. J. and Iedema P. D., *J. Chem. Phys.*, **122** (2005) 154503.
[16] Happel J. and Brenner H., *Low Reynolds Number Hydrodynamics* (Kluwer Academic, Dordrecht) 1991.
[17] Dent G. L., PhD Thesis (1999) Brown University.
[18] Pivkin I. V. and Karniadakis G. E., *J. Comput. Phys.*, **207** (2005) 114.
[19] Pivkin I. V. and Karniadakis G. E., *Phys. Rev. Lett.*, **96** (2006) 206001.
[20] Filippov A. V., *J. Colloid Interface Sci.*, **229** (2000) 184.
[21] Geller A. S., Mondy L. A., Rader D. J. and Ingber M. S., *J. Aerosol Sci.*, **24** (1993) 597.